Mem. S.A.It. Suppl. Vol. 17, 122

Memorie della
Supplementi

The evolution of star forming galaxies with the Wide Field X-ray Telescope

P. Ranalli

Università di Bologna – Dipartimento di Astronomia, via Ranzani 1, 40127 Bologna, Italy
e-mail: piero.ranalli@oabo.inaf.it

Abstract. Star forming galaxies represent a small yet sizable fraction of the X-ray sky (1%–20%, depending on the flux). X-ray surveys allow to derive their luminosity function and evolution, free from uncertainties due to absorption. However, much care must be put in the selection criteria to build samples clean from contamination by AGN. Here we review the possibilities offered by the proposed WFXT mission for their study. We analyze the expected luminosity and redshift distributions of star forming galaxies in the proposed WFXT surveys. We discuss the impact of such a mission on the knowledge of the cosmic star formation history, and provide a few suggestions.

Key words. X-rays: galaxies – galaxies: luminosity function – galaxies: evolution – galaxies: high-redshift – galaxies: spiral

1. Introduction

The X-ray luminosity of star forming galaxies (SFG; they usually are spiral galaxies without AGN activity) appears to be a reliable, absorption-free estimator of star formation (Ranalli et al. 2003). This is justified on the basis that the X-ray luminosities are linearly and tightly correlated with the radio and FIR ones, which in turn are commonly used as star formation rate (SFR) indicators. Thus, the X-ray emission of SFG may be considered as a tool to investigate the cosmic star formation history. To this end, the study of the X-ray luminosity function (XLF) of galaxies and of its evolution represents a necessary step. Ranalli et al. (2005, hereafter RCS05) built a local ($z = 0$) XLF of SFG and investigated the possibilities for evolution. In this paper, we build on the RCS05 XLF and methods to explore the possible contribution of the Wide Field X-ray Telescope (WFXT) mission to our understanding of the SFG content of the universe, by analyzing the expected luminosity and redshift distributions.

The WFXT is a proposed mission which aims to perform very wide and moderately deep X-ray surveys. By taking a different approach to mirror design than the classical Wolter type-1 (Burrows et al. 1992), it could achieve a very large field of view ($\sim$ 1 deg^2) while maintaining a good angular resolution ($\sim 5''$) and a large effective area ($\sim$ 1 m^2) in the 0.1-7 keV band (Conconi et al. 2010).

Such a telescope would be able to observe a number of X-ray sources far exceeding all those known today. While X-ray surveys mainly detect AGN, star-forming galaxies (SFG) are also present, comprising a frac-

Send offprint requests to: P. Ranalli

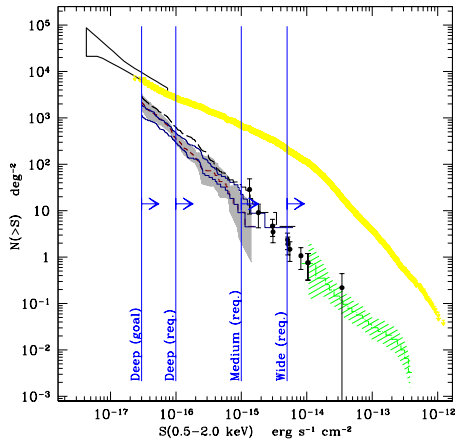

Fig. 1. Observed X-ray number counts in today's surveys, and planned WFXT limiting fluxes. The thick upper line and the horn show the observed Log N–Log S for all X-ray sources in the *Chandra* Deep Fields (Moretti et al. 2003) and the limits from the fluctuation analysis (Miyaji & Griffiths 2002). The bundle of histograms and data points shows several determinations of the star-forming galaxies Log N–Log S (see text). The vertical lines illustrate the limiting fluxes of the planned surveys.

Table 1. Covered area (deg^2) and limiting fluxes (erg s^{-1} cm^{-2} in the 0.5–2.0 keV band) of the proposed WFXT surveys.

	wide	medium	deep
area	20000	3000	100
flux (req.)	$5 \cdot 10^{-15}$	10^{-15}	10^{-16}
flux (goal)	$3 \cdot 10^{-15}$	$5 \cdot 10^{-16}$	$3 \cdot 10^{-17}$

tion in the range 1%–20% (depending on the flux) of all the sources detected in the 0.5–2.0 keV band. Three major surveys are envisaged with the WFXT, covering different amounts of the sky at different limiting fluxes and named *wide*, *medium* and *deep* (Fig 1). Their limiting soft X-ray fluxes correspond broadly to those probed in ROSAT (Tajer et al. 2005), XMM-*Newton* (Georgakakis et al. 2004) and deep *Chandra* (Bauer et al. 2004; Norman et al. 2004, RCS05) surveys of SFG. In Fig. 1 we show the total Log N–Log S from X-ray surveys, and different estimates of the SFG number counts.

Depending on technological developments, both a *requirement* and a *goal* value for the limiting fluxes can be quoted. Reaching the goals could extend the number of detected objects by a factor ~ 5. However, given the early stage of the mission, here we will consider only the requirements, and regard the goal flux limit for the *deep* survey only.

We assume $H_0 = 70$ km s^{-1} Mpc^{-1}, $\Omega_{\rm M} = 0.3$ and $\Omega_\Lambda = 0.7$.

2. The LF and evolution of star-forming galaxies

The local differential luminosity function

$$\varphi(\mathrm{Log}L)\,\mathrm{dLog}L \tag{1}$$

is defined as the comoving number density of sources per logarithmic luminosity interval. The evolution can be described as pure luminosity with the form (Schmidt 1972)

$$L(z) \propto (1+z)^{\eta_{\rm l}}. \tag{2}$$

Infrared surveys provide a powerful method to select SFG, since the bulk of the far and near IR emission is due to reprocessed light from star formation, with AGN representing only a minor population (de Jong et al. 1984; Franceschini et al. 2001; Elbaz et al. 2002). The FIR LFs may be assumed to be essentially unaffected by a contribution from Seyfert galaxies, as the fraction of Seyferts is about $\sim$ 5–10% (RCS05). While many determinations of IR LFs exist (see references in RCS05), here we take Takeuchi et al. (2003, 2004, hereafter T03) as reference. This is a 60μ LF derived from the IRAS Point Source Catalog Redshift (Saunders et al. 2000) (PSCz). It includes 15,411 galaxies with $z \lesssim 0.07$, covering 84% of the sky with a flux limit of 0.6 mJy at 60μ. While T03 reports pure-density evolution for their LF, pure-luminosity may provide an equally good fit to the data (T. Takeuchi, priv. comm.).

Other determinations of the SFG LF have been derived by the cross correlation of radio surveys with optical ones (see references in RCS05). The redshifts covered in these surveys are similar to those of the T03 galaxies,

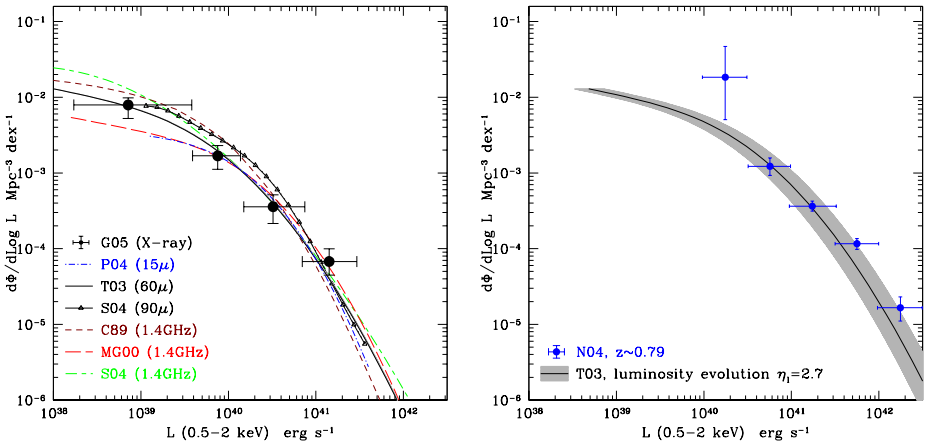

Fig. 2. *Left:* IRAS, ISO, and radio local luminosity functions of SFG converted to the X-rays (see RCS05 for references to the individual LFs). All the LFs converge to the same location. The large data points with error bars show an observational determination of the local XLF, based on XMM-*Newton* data by Georgantopoulos et al. (2005). *Right:* Comparison of the XLF derived from IRAS data (solid curve; the grey area shows the uncertainty on the evolution) with the XLF derived by Norman et al. (2004) in the *Chandra* Deep Field (data points with error bars).

but the number of objects is smaller due to a smaller sky coverage, so reliable estimates of the evolution may not be derived.

The local IR or radio LFs may be converted to X-ray ones by using the approach first developed in Avni & Tananbaum (1986) (see also: Georgantopoulos et al. 1999; Norman et al. 2004), which may be summarised as follows. Given a galaxy with IR or radio luminosity L, let $P(L_{\rm X}|L)$ be the probability distribution of the possible values of the galaxy's X-ray luminosity $L_{\rm X}$, as given by the optical/IR/radio vs. X-ray correlations. Thus, the X-ray LF may be otained by the convolution of an optical/IR/radio LF with $P(L_{\rm X}|L)$. In Ranalli et al. (2003) it was reported that the X-ray luminosity is tightly correlated with radio and FIR luminosities. By assuming a Gaussian probability distribution for these correlations, one has for example

$$P(\mathrm{Log}\, L_{0.5-2\mathrm{keV}}|\, \mathrm{Log}\, L_{60\mu}) = \\ = \frac{1}{\sqrt{2\pi}\sigma}\, \mathrm{e}^{-\frac{\mathrm{Log}\, L_{60\mu}+9.05-\mathrm{Log}\, L_{0.5-2}}{2\sigma^2}} \qquad (3)$$

with $\sigma \sim 0.30$.

A clear prediction for a $z = 0$ XLF emerges from the comparison of the infrared and radio LFs (Fig. 2, left panel): the derived XLFs agree within a factor of 2 in the luminosity interval 10^{40}–10^{41} erg s^{-1}, encompassing the knee region after which all XLFs steepen toward higher luminosities; although departures at lower and higher luminosities are present, the average local X-ray luminosity density, $\sim (3 \cdot 10^{37} \pm 30\%)$ erg s^{-1} Mpc^{-1}, appears to be well defined.

Norman et al. (2004) derived an XLF at higher redshifts (two bins: $\bar{z} \sim 0.27$ and $\bar{z} \sim 0.79$; Fig. 2, right panel) than those probed by the IR and radio surveys discussed above. Other strong constraints at high redshift come from the COMBO-17 survey (Wolf et al. 2003), and from the comparison of the observed X-ray Log N–Log S with that derived by integrating the XLF. This work has been done in detail in RCS05, and here we just quote the results: the evolution is well described as pure-luminosity with an exponent $\eta_{\rm l} \sim 2.7$, with possibly an hint that the evolution could be stopped at $z \sim 1$ (Fig. 2, right panel).

3. Expected luminosity and redshift distributions with the WFXT

The XLF derived in the previous section can be integrated in the volume of space probed by the surveys to obtain luminosity distributions

$$\frac{\mathrm{d}N}{\mathrm{dLog}L} = \int_0^{z_{\max}} \varphi(\mathrm{Log}L, z')\ \min[V(z), V(\mathrm{Log}L, F_{\lim})]\ \mathrm{d}z \qquad (4)$$

and redshift distributions

$$\frac{\mathrm{d}N}{\mathrm{d}z} = \int_{\mathrm{Log}L_{\min}}^{\mathrm{Log}L_{\max}(z')} \varphi(\mathrm{Log}L, z')\ \min[V(z), V(\mathrm{Log}L, F_{\lim})]\ \mathrm{dLog}L \qquad (5)$$

where $z' = \min(z, z_{\mathrm{stop}})$; $F_{\lim}$ is the limiting flux of the survey; $V(z)$ is the comoving volume at redshift z; and $V(L, F)$ is the comoving volume at the redshift at which a source with luminosity L is observed with flux F. All fluxes are considered in the 0.5–2.0 keV band.

For the following calculations, we take $z_{\max} = 4$, $z_{\mathrm{stop}} = 1$, $L_{\min} = \max[10^{39}, 4\pi \mathrm{D}_{\mathrm{lum}}(z)^2 F_{\lim}]$ erg s^{-1} and $L_{\max} = 10^{42}(1 + z')^{\eta_{\mathrm{l}}}$ erg s^{-1}. In words, this means that we integrate on the luminosity range (at $z = 0$) 10^{39}–10^{42} erg s^{-1}, that we allow the maximum luminosity to evolve with redshift, that we exclude luminosities lower than what could visible given the redshift and limiting flux, and that the integration is done up to $z = 4$ but stopping the evolution at $z_{\mathrm{stop}} = 1$. The evolution is pure-luminosity as in Eq. (2) with $\eta_{\mathrm{l}} = 2.7$.

The luminosity distribution is shown in Fig. 3, both in cumulative (left panel) and differential form (right panel). The cumulative form immediately shows the total number of SFG which are expected to be detected in the WFXT surveys ($2 \cdot 10^4$–$4 \cdot 10^4$ objects per survey). Reaching the development goal would enhance the number of SFG by a factor of ~ 5, up to $2 \cdot 10^5$ objects in the *deep* survey.

It is important to check that the SFG XLF will be well sampled at all luminosities. From Fig. 3 it is evident that at least 10^3 SFG with $L < 2 \cdot 10^{39}$ erg s^{-1} should be detected in the *medium* and *deep* surveys, and that the "knee" region of the XLF (the range 10^{40}–10^{41} erg s^{-1} at $z = 0$, compare with Fig. 2) will be very well sampled with around $1.6 \cdot 10^4$ objects in each of the *medium* and *deep* surveys. Similarly, the high luminosity tail ($L > 10^{42}$ erg s^{-1}) will also be well sampled with around $7 \cdot 10^3$ objects in the *medium* survey. This part of the XLF is especially important because objects in this luminosity range are quite rare, and generally suspected of having a substantial part of their emission due to an AGN. Refined classification criteria, and the possibility of doing spectral analysis will clearly be essential.

Reaching the development goal will enlarge the sample of SFG with $L < 10^{42}$ erg s^{-1} by a factor of ~ 5, while it should not make much difference for brighter objects.

The expected redshift distribution is shown in Fig. 4 (left panel). The *wide* and *medium* surveys should have redshift peaks around 0.02 and 0.05, respectively. Both will provide sizable samples at larger redshift: ~ 1000 in the range $0.2 < z < 0.3$ for the *wide* survey, and ~ 900 in the range $0.6 < z < 0.7$ for the *medium*. The *deep* survey will probe much higher redshifts: ~ 900 objects with $1.2 < z < 1.3$, and other ~ 900 with $1.5 < z < 2.0$; these numbers would also be larger by a factor of ~ 5, if the development goal is reached. The uncertainties on the SFG evolution are illustrated by the grey area in Fig. 4 (left panel), whose upper and lower edges correspond to evolution with $\eta_{\mathrm{l}} = 3.4$ and 2.0, respectively.

However, it is likely that the highest redshift objects will also have the larger luminosities. Thus it is reasonable to ask *up to which redshift will the knee of the XLF be probed*. The local XLF exhibits its knee in the range 10^{40}–10^{41} erg s^{-1} (Fig. 2), thus we repeated the integration in Eq. (5) taking $L_{\max} = 3 \cdot 10^{40}(1+z')^{\eta_{\mathrm{l}}}$ erg s^{-1}. The result is shown in Fig. 4 (right panel). The *wide* and *medium* surveys will not probe the knee of the XLF at redshift larger than $z \sim 0.1$ and $z \sim 0.2$, respectively. The *deep* survey will extend the probed redshift range up to $z \sim 0.5$, while if the development goal is reached, redshifts as large as ~ 1.1 could be observed.

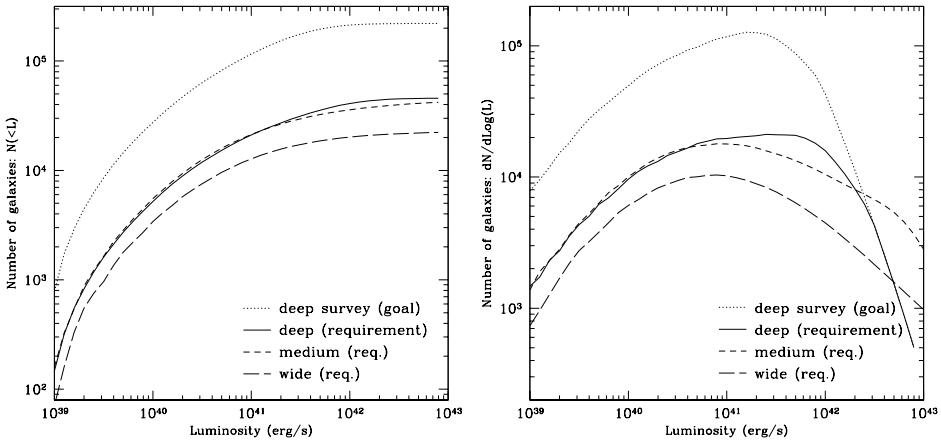

Fig. 3. *Left:* Expected cumulative luminosity distributions for SFG in the WFXT surveys. *Right:* Differential luminosity distributions. Since the knee of the SFG XLF is comprised (at $z = 0$) in the range 10^{40}–10^{41} erg s^{-1}, it appears that the XLF will be well sampled by the WFXT.

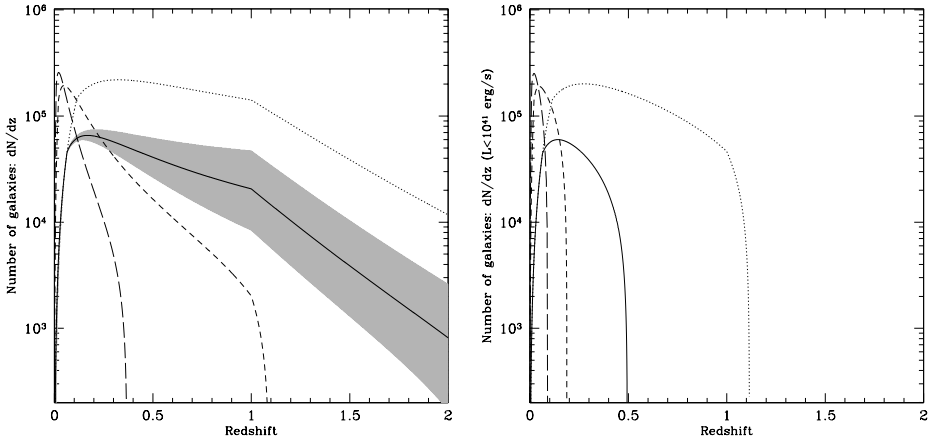

Fig. 4. *Left:* Expected differential redshift distributions for SFG in the WFXT surveys. The grey area illustrates how the uncertainties about the XLF evolution could affect the *deep* survey. *Right:* Same as left, but only considering galaxies with luminosity $L \leq 3 \cdot 10^{40}(1 + z')^{\eta}$ erg s^{-1}: the knee region of the XLF will be probed up to $z \sim 0.5$–1.1. *Both:* Line styles as in Fig. 3.

4. Discussion

From the expected luminosity and redshift distributions, it is evident that the WFXT will be able to determine the SFG XLF with an accuracy comparable to that of IRAS or optical surveys. Thus there will be many new possibilities to study how the X-ray emission depends on other parameters, such as morphology, colours, redshift, etc. However, such a work could only be made if multiwavelength information is available. In fact, the first and most important task will be the selection of the SFG, which are a minor fraction of the total of X-ray surveys. Several different combinations of the same basic parameters (X-ray lu-

minosity, X-ray/optical flux ratio, hardness ratio, amount of absorption, presence of broad lines in optical spectra, etc.) have been explored by different authors in deep *Chandra* surveys (RCS05, and references therein). All the determinations differ by up to a factor of $\sim$ 2; this scatter can be reduced only with a better understanding of how these parameters are linked to each other, and how they affect the selection (and the completeness of samples) of SFG. This only gets more difficult for wide-and-shallow surveys (respect to deep pencil-beam ones) because the SFG/AGN fraction in X-ray surveys depends on the limiting flux (Fig. 1). An attempt to investigate this problem for a sample of SFG in the *Chandra*-COSMOS survey (Elvis et al. 2009) may be found in Ranalli et al. (2010, to be submitted). One of its main results is that no rigid boundaries on the selection parameters can be put; a sensible approach should build on statistical methods for object classification.

The need for the most complete multiwavelength coverage also requires that the choice of the sky areas covered by the WFXT surveys be coordinated with (or follow, if not possible otherwise) other present and future survey facilities (Pan-Starrs, the Large Synoptical Survey Telescope, ALMA, LOFAR, E-VLA, etc.).

The planned WFXT surveys will be able to derive the SFG XLF and determine its evolution with unprecedented accuracy up to $z \sim 0.5$ (1.1 if the development goals are reached) in the knee region, and up to $z \sim 2$ (2.5) for the high-luminosity tail. Since the cosmic star formation history as a peak in the range $1 \lesssim z \lesssim 2$, it is evident that the goals should be pursued with strong commitment. The cosmic accretion history has a peak at a similar redshift, and the two phenomena seem to have shared a very similar trend. Thus, the larger the probed redshift range, the more impact the WFXT will have for studies of SFG and AGN coevolution.

Finally, were the goals reached, and the numbers still on the safe side of the confusion limit, some ultra-deep pointings should be considered as very profitable. E.g., observing an area of 10 deg^2 with a limiting flux of 10^{-17} erg s^{-1} cm^{-2} would extend the coverage of the knee of the XLF up to $z \sim 1.7$, and of the high-luminosity tail up to redshifts well beyond the peak of the cosmic star formation history.

Acknowledgements. We thank Roberto Gilli and Andrea Comastri for stimulating discussions.

References

Avni, Y. & Tananbaum, H. 1986, ApJ, 305, 83
Bauer, F. E., Alexander, D. M., Brandt, W. N., et al. 2004, AJ, 128, 2048
Burrows, C. J., Burg, R., & Giacconi, R. 1992, ApJ, 392, 760
Conconi, P., Campana, S., Tagliaferri, G., et al. 2010, MNRAS, 509
de Jong, T., Clegg, P. E., Rowan-Robinson, M., et al. 1984, ApJ, 278, L67
Elbaz, D., Cesarsky, C. J., Chanial, P., et al. 2002, A&A, 384, 848
Elvis, M., Civano, F., Vignali, C., et al. 2009, ApJS, 184, 158
Franceschini, A., Aussel, H., Cesarsky, C. J., Elbaz, D., & Fadda, D. 2001, A&A, 378, 1
Georgakakis, A. E., Georgantopoulos, I., Basilakos, S., Plionis, M., & Kolokotronis, V. 2004, MNRAS, 354, 123
Georgantopoulos, I., Basilakos, S., & Plionis, M. 1999, MNRAS, 305, L31
Georgantopoulos, I., Georgakakis, A., & Koulouridis, E. 2005, MNRAS, 360, 782
Miyaji, T. & Griffiths, R. E. 2002, ApJ, 564, L5
Moretti, A., Campana, S., Lazzati, D., & Tagliaferri, G. 2003, ApJ, 588, 696
Norman, C., Ptak, A., Hornschemeier, A., et al. 2004, ApJ, 607, 721
Ranalli, P., Comastri, A., & Setti, G. 2003, A&A, 399, 39
Ranalli, P., Comastri, A., & Setti, G. 2005, A&A, 440, 23
Saunders, W., Sutherland, W. J., Maddox, S. J., et al. 2000, MNRAS, 317, 55
Schmidt, M. 1972, ApJ, 176, 273
Tajer, M., Trinchieri, G., Wolter, A., et al. 2005, A&A, 435, 799
Takeuchi, T. T., Yoshikawa, K., & Ishii, T. T. 2003, ApJ, 587, L89
Takeuchi, T. T., Yoshikawa, K., & Ishii, T. T. 2004, ApJ, 606, L171
Wolf, C., Meisenheimer, K., Rix, H.-W., et al. 2003, A&A, 401, 73